Mon. Not. R. Astron. Soc. **000**, 1–11 (2002) Printed 5 February 2008 (MN LaTeX style file v2.2)

arXiv:astro-ph/0606707v1 29 Jun 2006

Radio and X-ray Properties of Relativistic Beaming Models for Ultra-Luminous X-ray Sources

M. Freeland[1⋆], Z. Kuncic[1⋆], R. Soria[2,3⋆], and G. V. Bicknell[4⋆]
[1] *School of Physics, University of Sydney, NSW 2006, Australia*
[2] *Harvard-Smithsonian Centre for Astrophysics, Cambridge, MA 02138, USA*
[3] *Mullard Space Science Laboratory, University College London, Holmbury St Mary, Dorking, RH5 6NT, UK*
[4] *Research School of Astronomy & Astrophysics, Australian National University, ACT 2611, Australia*

Accepted 1988 December 15. Received 1988 December 14; in original form 1988 October 11

ABSTRACT

We calculate the broadband radio–X-ray spectra predicted by microblazar and microquasar models for Ultra-Luminous X-ray sources (ULXs), exploring the possibility that their dominant power-law component is produced by a relativistic jet, even at near-Eddington mass accretion rates. We do this by first constructing a generalized disk–jet theoretical framework in which some fraction of the total accretion power $P_{\rm a}$ is efficiently removed from the accretion disk by a magnetic torque responsible for jet formation. Thus, for different black hole masses, mass accretion rates and magnetic coupling strength, we self-consistently calculate the relative importance of the modified disk spectrum, as well as the overall jet emission due to synchrotron and Compton processes. In general, transferring accretion power to a jet makes the disk fainter and cooler than a standard disk at the same mass accretion rate; this may explain why the soft spectral component appears less prominent than the dominant power-law component in most bright ULXs. We show that the apparent X-ray luminosity and spectrum predicted by the microquasar model are consistent with the observed properties of most ULXs. We predict that the radio synchrotron jet emission is too faint to be detected at the typical threshold of radio surveys to date. This is consistent with the high rate of non-detections over detections in radio counterpart searches. Conversely, we conclude that the observed radio emission found associated with a few ULXs cannot be due to beamed synchrotron emission from a relativistic jet.

Key words: accretion, accretion disks – black hole physics – X-rays: binaries – relativistic jets.

1 INTRODUCTION

Ultra-Luminous X-ray sources (ULXs) are among the most intriguing sources to have been discovered by X-ray satellites. They are defined as point-like X-ray sources which, if located within the galaxy they are associated with on the sky, are off-nuclear and have X-ray luminosities $L_{0.5-8\,{\rm keV}} \gtrsim 2 \times 10^{39}\,{\rm erg\,s^{-1}}$ in the $0.5 - 8.0\,$keV bandpass (Irwin, Bregman & Athey 2004). This exceeds the theoretical Eddington limit for a neutron star or stellar-mass black hole, $L_{\rm Edd} = 4\pi G M_{\rm bh} \mu m c/\sigma_{\rm T}$, where $M_{\rm bh}$ is the black hole mass and μ is the mean molecular weight. It also exceeds the peak in observed X-ray luminosities of known Galactic X-ray binaries (XRBs). Spectroscopic studies have revealed that some ULXs can be identified with supernova remnants or background AGN (see e.g. Gutiérrez & López-Corredoira 2005, and references therein). Of the remaining unidentified sources, however, rapid X-ray variability (e.g. Strohmayer & Mushotzky 2004; Soria & Motch 2004; Krauss et al. 2005) and spectral state transitions (Kubota et al. 2001; Kubota, Done & Makishima 2002; La Parola et al. 2001; Mizuno, Kubota & Makishima 2001; Strickland et al. 2001) strongly suggest that we are dealing with a population of close interacting binary systems involving accretion onto a black hole.

Perhaps the most contentious issue surrounding ULXs is the mass of the black hole, $M_{\rm bh}$, which determines $L_{\rm Edd}$. There are at least three possible explanations for why many ULXs are apparently $\sim 20 - 30$ times more luminous than typical Galactic black hole XRBs: 1. The emission is Doppler-boosted by a relativistic jet pointing towards

---

⋆ E-mail: mcf35@cam.ac.uk, z.kuncic@physics.usyd.edu.au, rs1@mssl.ucl.ac.uk, geoff@mso.anu.edu.au

us (microblazar scenario: e.g. Fabrika & Mescheryakov 2001; Körding, Falcke & Markoff 2002). In this case, $M_{\rm bh}$ need not be more than $\sim$ a few $M_\odot$, similar to typical stellar-mass black holes in the Galaxy. 2. The brightness enhancement is due to a combination of various factors: mild beaming, $M_{\rm bh}$ more massive than typical Galactic sources, and super-Eddington accretion. A factor of ~ 3 for each of these terms is physically plausible and would suffice for most ULXs (e.g. King & Dehnen 2005). In particular, mild geometric beaming could result from a sub-relativistic, radiatively-driven disk outflow (King et al. 2001; King 2004). Alternatively, it could be the result of a relativistic jet pointing slightly away from us (microquasar scenario). 3. The X-ray emission is isotropic and Eddington-limited; the high luminosity arises from a more massive black hole (an intermediate-mass black hole, IMBH), with $M_{\rm bh} \sim 10^{2-3} M_\odot$ (Colbert & Mushotzky 1999; Makishima et al. 2000; Miller et al. 2003). In this case the X-ray source is truly ultra-luminous, and hence it requires an accretion rate higher than that for a beamed scenario. If ULXs were proven to be powered by an accreting IMBH, the implications would be far-reaching, impacting on many other fields, from star-formation to cosmology (see Miller & Colbert 2004 for a review).

In principle, phase-resolved optical spectroscopic and photometric studies are the most direct way to determine the binary system parameters (viewing angle, orbital period, radial velocity curve and hence, mass function – see e.g. Charles 1998) and constrain the nature of ULXs. This is how Galactic black holes were first identified. However, optical counterpart searches and phase-resolved studies have proven exceedingly difficult for ULXs because even the nearest ones are located at distances of a few Mpc. Moreover, the brightest ULXs tend to be preferentially located in crowded star forming regions (Irwin et al. 2004), making unambiguous optical identifications often impossible, even within the *Chandra* error circle. When optical counterparts are found, they are generally consistent with O or B0 stars (Liu et al. 2002, 2004; Kaaret et al. 2004; Zampieri et al. 2004). However, this could be a selection effect, since smaller donors (perhaps lower-mass stars evolving through their giant phase) would be too faint to be detected. Hence, it is important to identify the discriminating signatures of ULXs in other wavebands.

Radio observations may provide a more effective means of differentiating the isotropic IMBH and beaming models. By analogy with AGN, we can expect a ULX microblazar to produce strong synchrotron radio emission from a compact, unresolved core, while more extended, and possibly elongated and resolved radio structure may arise from a ULX microquasar, seen at larger inclination. To date, radio counterparts have been detected for only a few ULXs: two in M82 (Kronberg & Sramek 1985; Körding, Colbert & Falcke 2005); one in NGC 5408 (Kaaret et al. 2003; Soria et al. 2006a); one in Holmberg II (Tongue & Westpfahl 1995; Miller, Mushotzky & Neff 2005); one in NGC 7424 (Soria et al. 2006b); and one in NGC 6946 (van Dyk et al. 1994; Blair, Fesen & Schlegel, 2001; Swartz et al. 2006, in prep.). It is still unclear whether the emission in those radio sources is due to an underlying supernova remnant or is directly produced by ULX jet activity, either from the core or the lobes. Hence, it is important to determine the radio signatures of different ULX models.

In the X-ray band, ULX spectra are generally dominated by a power-law, particularly above 1 keV. A cool thermal component is present in some sources, but contributes at most $10-20\,\%$ of the flux (e.g. Stobbart, Roberts & Wilms 2006). A power-law component is also dominant in the X-ray spectra of Galactic black holes in two of the canonical spectral states (McClintock & Remillard 2006): the low/hard state, when the photon index is $\Gamma \sim 1.5-2$ and the X-ray luminosity is $L_{0.5-8\,{\rm keV}} \lesssim 10^{-2} L_{\rm Edd}$; and the very high (or steep power-law) state, when $\Gamma \gtrsim 2.5$ and $L_{0.5-8\,{\rm keV}} \sim L_{\rm Edd}$. In the low/hard state, the accretion disk is thought to be truncated far from the innermost stable circular orbit (ISCO), and replaced by a radiatively inefficient flow with a steady jet (see e.g. Esin et al. 1997). The very high state, on the other hand, is characterized by a high radiative efficiency, quasi-periodic X-ray variability, and absence of a steady jet, although flares or sporadic radio ejections are associated with this state. It is not clear whether ULXs can be classified into either one of these power-law dominated XRB states; their photon index is somewhat intermediate, with $\Gamma \approx 1.5-2.5$ (e.g. Swartz et al. 2004; Stobbart et al. 2006; Winter et al. 2006). If they are in a classical low/hard state, their apparent X-ray luminosities suggest masses $\gtrsim$ a few $\times\, 10^3 M_\odot$. What seems clear is that ULXs are not in a high/soft state, when the X-ray spectrum is dominated by soft disk blackbody emission and the power-law is weaker.

Regardless of which spectral state ULXs belong to, the power-law component could be produced either by thermal Comptonization in a hot, diffuse corona, or by nonthermal synchrotron and Compton processes in a relativsitic jet, or possibly a combination of both (see Markoff et al. 2003, for a discussion). Although it is widely accepted that relativistic jets are responsible for extragalactic radio sources, analogous jet models for Galactic XRBs have only been considered relatively recently (see Fender 2005, for a review). Existing disk-jet models for binaries, however, either neglect the radio synchrotron properties altogether (e.g. Georganopoulos, Aharonian & Kirk 2002) or are only appropriate for the low/hard state (e.g. Markoff, Falcke & Fender 2001; Markoff et al. 2003; Fender, Belloni, & Gallo 2004). It is important to explore the possibility of a jet coexisting with (and coupled to) a bright disk extending all the way down to the ISCO[1].

In this paper, we investigate both the radio and X-ray properties of relativistic beaming models for ULXs using an accreting black hole framework generalized to include coupled disk-jet spectral components. Specifically, the radio and hard X-ray emission are produced in a relativistic jet that is magnetically coupled to an accretion disk (which can contribute to the soft X-ray emission). The jet drains a substantial fraction of the total accretion power from the disk and thus modifies the multi-colour disk spectrum. In order to calculate the spectral energy distribution, we explicitly model the mechanism which magnetically couples the disk and jet. Thus, our generalized model calculates both the jet and disk spectra *self-consistently* for different values of the black hole mass $M_{\rm bh}$, mass accretion rate $\dot{M}_{\rm a}$, and coupling strength. This leads to two unique features of the model that have important implications not just for ULXs, but for all accreting systems: 1. The nett accretion power can exceed the Eddington limit because the jet efficiently channels energy from the disk, which remains sub-Eddington; and 2. The presence of a jet can be inferred indirectly from its effects on the disk, which consequently emits a spectrum that can be considerably different from that predicted by the standard Shakura-Sunyaev (Shakura & Sunyaev 1973) disk in the EUV/soft-X-ray bandpass for XRBs. Our coupled disk-jet theory is outlined in Sec. 2; results for beamed ULX models are presented in Sec. 3; and a discussion and conclusions are given in Secs. 4 and 5, respectively.

---

[1] Recent X-ray/radio studies of FRII radio galaxies and quasars (e.g. Punsly & Tingay 2005; Ballantyne & Fabian 2005) provide examples of powerful nuclear jets co-existing with a high luminosity spectral state ($L_{\rm X} \sim L_{\rm Edd}$).

2 THEORETICAL BASIS

The model we construct here is based on the generalized accretion disk theory of Kuncic & Bicknell (2004), which gives self-consistent solutions for the radiative flux of a turbulent, magnetized accretion disk modified by an outflow that could be either mass-flux or Poynting-flux dominated. A mass-flux dominated outflow requires $\dot{M}_{\rm a}$ to vary with radius r in the disk. We restrict ourselves here to modelling a Poynting-flux dominated outflow. The solutions also take into account the possibility of a non-zero magnetic torque acting on the inner boundary, although we do not consider this effect here. We calculate an outflow-modified multi-colour-disk (OMMCD) spectrum, assuming each annulus is locally emitting a blackbody. A Newtonian potential is used.

The fraction of accretion power removed from the disk by the magnetic torque acting on the surface is channelled into the jet and partitioned into kinetic energy (bulk and random), magnetic field, and radiative energy components. We calculate the jet spectrum due to synchrotron, synchrotron self-Comptonization (SSC) and inverse Compton (IC) scattering of the disk photons by the energetic electrons in the jet. We test the micro-blazar/quasar models for ULXs by comparing the theoretical spectra for different values of $M_{\rm bh}$, $\dot{M}_{\rm a}$, jet power $P_{\rm j}$ and inclination angle $\theta_{\rm i}$ measured relative to the jet axis.

2.1 Modified disk emission

Assuming a zero nett torque at the inner disk boundary $r_{\rm i}$ and no radial variations in the mass accretion rate $\dot{M}_{\rm a}$ due to a mass-loaded wind, the radiative flux of a magnetized accretion disk with a non-zero magnetic torque acting on the disk surface is (Kuncic & Bicknell 2004, 2006, in preparation)

$$F_{\rm d}(r) = \frac{3GM_{\rm bh}\dot{M}_{\rm a}}{8\pi r^3}\left[f_{\rm ss}(r) - f_{\rm j}(r)\right] \qquad , \qquad (1)$$

where $f_{\rm ss}(r)$ is the small-r correction term in the standard Shakura-Sunyaev (SS) disk theory, given by (Shakura & Sunyaev 1973)

$$f_{\rm ss} = 1 - \left(\frac{r}{r_{\rm i}}\right)^{-1/2} \qquad . \qquad (2)$$

The term $f_{\rm j}(r)$ is the jet correction factor due to a non-zero magnetic torque on the disk surface:

$$f_{\rm j}(r) = \frac{1}{\dot{M}_{\rm a}\Omega r^2}\int_{r_{\rm i}}^{r} 4\pi r^2 \frac{B_\phi^+ B_z^+}{4\pi}\,{\rm d}r \qquad , \qquad (3)$$

where B_ϕ^+ and B_z^+ are the azimuthal and vertical components of the local magnetic field, evaluated at the disk surface, and $\Omega = (GM_{\rm bh}/r^3)^{1/2}$ is the Keplerian orbital velocity.

We assume a power-law radial profile for the magnetic stress, *viz.*

$$\frac{B_\phi^+(r)B_z^+(r)}{4\pi} = \frac{B_\phi^+(r_{\rm i})B_z^+(r_{\rm i})}{4\pi}\left(\frac{r}{r_{\rm i}}\right)^{-q} \qquad (4)$$

and we require $q \gtrsim 2$ so that the total work done against the disk surface by the magnetic torque remains finite. The normalization of the magnetic stress is determined from global energy conservation, which requires

$$L_{\rm d} = P_{\rm a} - P_{\rm j} \qquad , \qquad (5)$$

where

$$L_{\rm d} = 2\int_{r_{\rm i}}^{\infty} 2\pi r F_{\rm d}(r)\,{\rm d}r \qquad (6)$$

is the disk radiative power,

$$P_{\rm a} = \int_{r_{\rm i}}^{\infty} 4\pi r \frac{3GM_{\rm bh}\dot{M}_{\rm a}}{8\pi r^3} f_{\rm ss}(r)\,{\rm d}r = \frac{1}{2}\frac{GM_{\rm bh}\dot{M}_{\rm a}}{r_{\rm i}} \qquad (7)$$

is the total accretion power, and

$$P_{\rm j} = \int_{r_{\rm i}}^{\infty} 4\pi r \frac{3GM_{\rm bh}\dot{M}_{\rm a}}{8\pi r^3} f_{\rm j}(r)\,{\rm d}r \qquad (8)$$

is the total jet power. Thus, the magnitude of the magnetic stress at $r_{\rm i}$ can be related to the fraction $P_{\rm j}/P_{\rm a}$ of total accretion power channelled into the jet, and substitution into (3) then yields

$$f_{\rm j}(r) = \frac{1}{2}\left(\frac{P_{\rm j}}{P_{\rm a}}\right)\left(\frac{q-\frac{3}{2}}{q-3}\right)\left(\frac{r}{r_{\rm i}}\right)^{-1/2}\left[1 - \left(\frac{r}{r_{\rm i}}\right)^{(3-q)}\right] \qquad (9)$$

For the specific case $q = 2.5$, this simplifies to $f_{\rm j} = (P_{\rm j}/P_{\rm a})f_{\rm ss}$ and hence, the disk flux is just $F_{\rm d}(r) = (3GM_{\rm bh}\dot{M}_{\rm a}/8\pi r^3)f_{\rm ss}(1 - P_{\rm j}/P_{\rm a})$, which has the same radial dependence as the SS disk.

The total disk spectrum is calculated assuming local blackbody emission, B_ν, at each r:

$$L_{{\rm d},\nu} = \int_{r_{\rm i}}^{\infty} 4\pi^2 r B_\nu[T(r)]\,{\rm d}r \qquad , \qquad (10)$$

where $T(r) = [F_{\rm d}(r)/\sigma]^{1/4}$ is the effective disk temperature at each radius and σ is the Stefan–Boltzmann constant. For a disk inclined at an angle $\theta_{\rm i}$ with respect to an observer's line-of-sight, the apparent luminosity spectrum is $L^{\rm obs}_{{\rm d},\nu} = \frac{1}{2}\cos\theta_{\rm i} L_{{\rm d},\nu}$. The effective temperature may not be directly observable; what is typically fitted to the data is the colour temperature, which is approximately equal to the effective temperature T multiplied by a spectral hardening factor ξ. Values of $\xi \sim 1.7 - 2.6$ have been suggested for Galactic black hole XRBs (e.g. Merloni et al. 2000; Makishima et al. 2000; Shrader & Titarchuk 2003). It has been suggested (Fabian, Ross & Miller 2004) a spectral correction factor $\xi \approx 1.7$ may be appropriate for the thermal disk fits to ULX spectra.

Figure 1 shows plots of $T(r)$ and $L_{\mathrm{d},\nu}$ predicted by our OMMCD model for $M_{\mathrm{bh}} = 5M_{\odot}$, $q = 2.6$, $P_{\mathrm{a}}/L_{\mathrm{Edd}} = 1$ and increasing values of $P_{\mathrm{j}}/P_{\mathrm{a}}$. We have integrated to an outer disk radius $r_{\mathrm{o}} = 10^3 r_{\mathrm{i}}$. The mass accretion rate is $\dot{M}_{\mathrm{a}} = (8\pi m_{\mathrm{p}} c r_{\mathrm{i}}/\sigma_{\mathrm{T}})(P_{\mathrm{a}}/L_{\mathrm{Edd}}) \simeq 8 \times 10^{-7}(r_{\mathrm{i}}/6r_{\mathrm{g}})(M_{\mathrm{bh}}/5M_{\odot})(P_{\mathrm{a}}/L_{\mathrm{Edd}})\, M_{\odot}\,\mathrm{yr}^{-1}$. The value $q = 2.6$ is used to demonstrate how the change in radial flux profile affects the integrated spectrum. The OMMCD model predicts a decrease in the temperature profile at small radii, compared with the standard SS disk model (Fig. 1, top panel). Therefore, the peak in the integrated spectrum comes from larger radii and occurs at lower energies, for a given $\dot{M}_{\mathrm{a}}$, as $P_{\mathrm{j}}/P_{\mathrm{a}}$ increases. For a given accretion rate and black hole mass, the OMMCD spectrum appears softer and cooler than a standard disk, and its spectral slope can be flatter than the characteristic $\nu^{1/3}$ slope of a standard disk spectrum (Fig. 1, bottom panel). Physically, this occurs because the magnetic disk-jet coupling mechanism is strongest at small r; in the inner disk, more energy is removed from the disk and used to power a jet. Phenomenologically, this effect could be modelled in terms of a spectral hardening factor $\xi \lesssim 1$. It has the opposite effect as the hardening factor $\xi \sim 1.7 - 2.6$ sometimes introduced to account for Comptonization of disk emission (Makishima et al. 2000; Shrader & Titarchuk 2003).

Observationally, the OMMCD model predicts an anticorrelation between the maximum disk temperature, T_{in}, and the contribution of the hard power-law component, for a fixed L_{X}, M_{bh} and $\dot{M}_{\mathrm{a}}$. Therefore, it provides an alternative mechanism for producing cooler, fainter disks, having a somewhat similar effect as higher black hole masses and lower accretion rates. This may be relevant for the spectral fitting of some ULXs where an unusually soft X-ray component ($T_{\mathrm{in}} \lesssim 0.2\,\mathrm{keV}$) has been interpreted as disk emission from an IMBH (see e.g. Miller et al. 2003; Miller, Fabian & Miller 2004; but see also King & Pounds 2003; Crummy et al. 2005 and Gonçalves & Soria 2006 for alternative interpretations of this soft component). We defer a more detailed investigation of the implications of our OMMCD model for ULX mass estimates to future work (Soria & Kuncic 2006, in preparation).

More generally, taking into account disk cooling in the presence of a jet can be important for correct spectral fitting of ULXs as well as Galactic XRBs. We emphasize that in the OMMCD model, the inner disk is not truncated or replaced by a radiatively-inefficient flow; therefore, the gravitational energy of the inflow is not lost via advection but is mostly transferred to the jet and then partly radiated with a nonthermal spectrum in the *Chandra* or *XMM-Newton* energy band. Drainage of the disk power may explain why most ULXs seem to be dominated by a relatively hard power-law component in the X-ray band even at luminosities $\gtrsim 0.1 L_{\mathrm{Edd}}$; in fact, none of the brightest ULXs have ever been observed in a disk-dominated spectral state analagous to the high/soft state of Galactic XRBs (see Stobbart et al. 2006 for a more detailed discussion of this issue). We note that disk irradiation can be non-negligible when the jet emission is only weakly beamed (Markoff & Nowak 2004) and this may in part explain the range of T_{in} fits to observed ULX spectra.

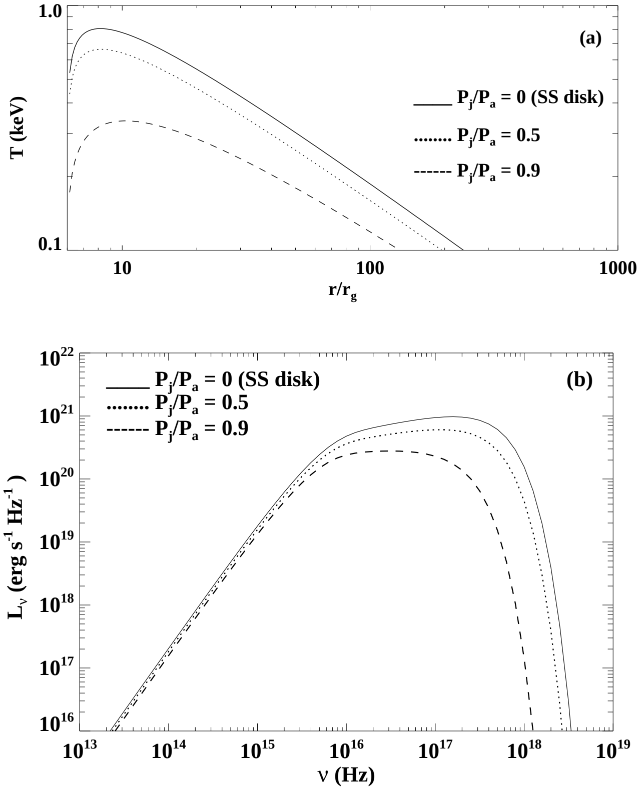

Figure 1. (a) Radial profile of the effective disk temperature, $T(r)$, for a standard Shakura-Sunyaev (SS) accretion disk (solid line), and for an outflow–modified disk with $P_{\mathrm{j}}/P_{\mathrm{a}}$ values of 0.5 (dotted) and 0.9 (dashed). (b) Luminosity spectra, $L_{\mathrm{d},\nu}$, for the standard SS multi-colour disk (MCD) and for the outflow-modified multi-colour disk (OMMCD). Linestyles are the same as in (a). The black hole mass is $M_{\mathrm{bh}} = 5M_{\odot}$, the mass accretion rate is $\dot{M}_{\mathrm{a}} \simeq 8 \times 10^{-7}\, M_{\odot}\,\mathrm{yr}^{-1}$ and the ratio of outer-to-inner disk radii is $r_{\mathrm{o}}/r_{\mathrm{i}} = 10^3$.

2.2 Jet emission

A fraction of the total power P_{j} channelled from the accretion flow in the form of Poynting energy is converted into kinetic energy. This is the basis for all disk-driven jet models (e.g. Blandford & Payne 1982). Thus, P_{j} can be partitioned into bulk and random particle energies, as well as magnetic energy (e.g. Celotti et al. 1998; Ghisellini & Celotti 2001):

$$P_{\mathrm{j}} = P_{\mathrm{bke}} + P_{\mathrm{e}} + P_{\mathrm{B}} \tag{11}$$

Some of the kinetic energy can also be subsequently dissipated in the form of radiation. However, for ultra-relativistic jets (in blazars, for instance) the total radiative output is usually negligible (see e.g. Celotti & Fabian 1993). The kinetic and magnetic energy components are then comoving with approximately constant speed β_{j} and bulk Lorentz factor $\Gamma_{\mathrm{j}} = (1 - \beta_{\mathrm{j}}^2)^{-1}$. We consider a conical, quasi-static jet with opening semi-angle ϕ_{j} and cross-sectional area πr_{j}^2, where $r_{\mathrm{j}} = z\phi_{\mathrm{j}}$ is the radius at a distance z along the jet axis.

The jet plasma is quasi-neutral, with one (cold) proton for each (relativistic) electron. The electrons are assumed to be continuously reaccelerated, maintaining a nonthermal power-law distribution $N_{\rm e}(\gamma) = K_{\rm e}\gamma^{-p}$ extending over energies $\gamma_{\rm min} \lesssim \gamma \lesssim \gamma_{\rm max}$ with an average value $\langle\gamma\rangle = \int N_{\rm e}(\gamma)\gamma\,{\rm d}\gamma/N_{\rm e}$, where $N_{\rm e}$ is the total electron number density. A quasi-steady jet requires a stochastic acceleration mechanism, such as second-order Fermi, in which the accelerating electrons continually scatter off small-scale inhomogeneities or MHD waves in the jet plasma; in contrast, non-steady jet behaviour can arise from localized acceleration sites at internal shocks (i.e. via first-order Fermi – see Sec. C7 in Begelman, Blandford & Rees 1984 for a detailed discussion on acceleration in jets). We use an equipartition relation $U_{\rm B} = f_{\rm eq}U_{\rm e}$ between the magnetic energy density $U_{\rm B} = B^2/8\pi$ and electron energy density $U_{\rm e} = N_{\rm e}\langle\gamma\rangle m_{\rm e}c^2$, where the equipartition factor $f_{\rm eq}$ remains constant along the jet.

The total jet power is approximately equal to the comoving kinetic and Poynting energy fluxes at the jet base z_0 (e.g. Celotti & Fabian 1993; Celotti et al. 1998; Schwartz et al. 2006):

$$\begin{aligned} P_{\rm j} &\simeq 2\pi r_{{\rm j},0}^2\Gamma_{\rm j}\beta_{\rm j}c\Big[(\Gamma_{\rm j}-1)N_{{\rm e},0}m_{\rm p}c^2 \\ &+ \frac{4}{3}\Gamma_{\rm j}N_{{\rm e},0}\langle\gamma\rangle m_{\rm e}c^2 + \Gamma_{\rm j}\frac{B_0^2}{4\pi}\Big] \qquad (12) \end{aligned}$$

where the subscript '0' refers to quantities evaluated at z_0. This relation is used to determine the electron number density at the jet base, $N_{{\rm e},0}$. The factor of 2 takes into account that $P_{\rm j}$ powers two oppositely directed jets. We use $\phi_{\rm j} \simeq 1/\Gamma_{\rm j}$ for $\Gamma_{\rm j} > 1$, consistent with a freely expanding relativistic flow (Blandford & Königl 1979).

The emission spectrum is calculated by subdividing the conical jet into multiple segments of thickness $\Delta z \ll z$. There are contributions to the spectrum emitted by each segment from synchrotron radiation, synchrotron self-Comptonization (SSC) and inverse-Compton (IC) scattering of the disk photons. We assume the emission to be isotropic in the jet rest-frame. We utilise a simple radiative transfer prescription to account for synchrotron self-absorption. The self-Compton and inverse-Compton processes are assumed to be optically thin. We calculate the (single scattering) IC and SSC emissivities using the full Klein-Nishina cross-section (see Blumenthal & Gould 1970; Königl 1981; Ghisellini et al. 1985), although the decline is negligible in the $0.5-8$ keV bandpass of interest here. The optically-thin spectral index is $\alpha \equiv {\rm d}\log L_\nu/{\rm d}\log\nu = -\frac{1}{2}(p-1)$.

We use two different spectral models, depending on whether the jet is viewed at small or large inclination angles. For the microblazar model, the inclination of the line of sight to the jet axis is less than the jet cone-angle (i.e. $\theta_{\rm i} < \phi_{\rm j}$). In this case, the specific luminosity seen by an observer at rest is calculated by integrating the emissivities over the whole jet length $z_{\rm max}$:

$$\begin{aligned} L^{\rm obs}_{{\rm j},\nu_{\rm obs}} &\simeq \int_{z_0}^{z_{\rm max}} 4\pi\delta^2\Big\{\varepsilon^{\rm IC}_{\nu=\nu_{\rm obs}/\delta}+\varepsilon^{\rm SSC}_{\nu=\nu_{\rm obs}/\delta} \qquad (13) \\ &+ \varepsilon^{\rm syn}_{\nu=\nu_{\rm obs}/\delta}\exp\left[-\tau^{\rm obs}_{\nu_{\rm obs}}(z)\right]\Big\}\pi r_{\rm j}^2\,{\rm d}z \end{aligned}$$

where $\tau^{\rm obs}_{\nu_{\rm obs}}(z) = \delta^{-1}\kappa^{\rm syn}_{\nu=\nu_{\rm obs}/\delta}(z_{\rm max}-z)$ is the optical depth to synchrotron self-absorption and $\delta = [\Gamma_{\rm j}(1-\beta_{\rm j}\cos\theta_{\rm i})]^{-1}$ is the relativisitc Doppler factor (see e.g. Königl 1981; Lind & Blandford 1985; Ghisellini et al. 1993). For the microquasar model, we have $\theta_{\rm i} > \phi_{\rm j}$. In this case, the path length through a jet segment as seen by a comoving observer is $\Delta z/\cos\theta_{\rm i} \simeq r_{\rm j}(z)/\sin\theta_{\rm i}$. Assuming Δz is sufficiently small that the emissivities and synchrotron source function $S^{\rm syn}_\nu = \varepsilon^{\rm syn}_\nu/\kappa^{\rm syn}_\nu$ remain approximately constant along each path length, the observed specific luminosity is then

$$\begin{aligned} L^{\rm obs}_{{\rm j},\nu_{\rm obs}} &\simeq \sum_{z=z_0}^{z_{\rm max}} 4\pi\Big\{\delta^2\left[\varepsilon^{\rm IC}_{\nu=\nu_{\rm obs}/\delta}+\varepsilon^{\rm SSC}_{\nu=\nu_{\rm obs}/\delta}\right]\frac{r_{\rm j}}{\sin\theta_{\rm i}} \qquad (14) \\ &+ \delta^3 S^{\rm syn}_{\nu=\nu_{\rm obs}/\delta}\left[1-\exp\left(-\tau^{\rm obs}_{\nu_{\rm obs}}\right)\right]\Big\}\pi r_{\rm j}^2 \end{aligned}$$

where the synchrotron self-absorption optical depth is now $\tau^{\rm obs}_{\nu_{\rm obs}} = \delta^{-1}\kappa^{\rm syn}_{\nu=\nu_{\rm obs}/\delta}r_{\rm j}/\sin\theta_{\rm i}$.

We consider a nonuniform jet in which $N_{\rm e}$ decreases with height as $N_{\rm e}(z) \propto z^{-2}$ and hence, $B(z) \propto z^{-1}$ (since $f_{\rm eq}$ is constant), consistent with flux conservation. The nonuniformity in $N_{\rm e}$ and B means that different jet regions contribute to different parts of the broadband spectrum, with X-rays produced near the base and radio emission produced near the opposite end of the jet. Theoretical spectra predicted by this jet model are presented in the following section.

3 RESULTS

The input parameters in our model are: $M_{\rm bh}$, $\dot{M}_{\rm a}$ (parametrised by $P_{\rm a}/L_{\rm Edd}$), $P_{\rm j}/P_{\rm a}$ (which normalizes the magnetic coupling strength, c.f. eqns. 3 and 9), $\Gamma_{\rm j}$, p, $\gamma_{\rm min}$, $\gamma_{\rm max}$, $f_{\rm eq}$, z_0, $z_{\rm max}$ and $\theta_{\rm i}$. Some of these free parameters can be constrained by the observed X-ray and radio properties of ULXs. Firstly, we note that soft thermal components, when present in ULX spectra, contribute no more than $10-20\,\%$ to the total flux (e.g. Stobbart et al. 2006), so we set $P_{\rm j}/P_{\rm a} = 0.9$. Secondly, in the *Chandra* sample (Swartz et al. 2004), the average $0.5-8$ keV spectral index is $\alpha \simeq -0.7$, implying $p \simeq 2.4$. Note, however, that the distribution of α in this sample appears to be approximately Gaussian and extends down to values of $\alpha \simeq 0.0$.

To investigate the radio properties of ULXs, we note that the specific luminosity of a radio source with flux density S_ν at a distance D is $L_\nu \simeq 1.2\times10^{24}\,(S_\nu/{\rm mJy})\,(D/{\rm Mpc})^2\,{\rm erg\,s^{-1}\,Hz^{-1}}$. Radio sources found to be spatially associated with ULXs all have radio spectral powers well above $10^{24}{\rm erg\,s^{-1}\,Hz^{-1}}$, while for other nearby ULXs studied by Körding et al. (2005), no radio counterparts have been found down to a detection limit of $10^{24}{\rm erg\,s^{-1}\,Hz^{-1}}$. We shall therefore take $L_\nu = 10^{24}{\rm erg\,s^{-1}\,Hz^{-1}}$ as an empirical threshold and determine whether either of the micro-blazar/quasar models can produce radio emission above this level. If the radio jet emission predicted by these models does not exceed the threshold for plausible parameters, then the observed radio sources must have other interpretations (e.g. radio lobes, SNR).

We consider cases with an equipartition factor $f_{\rm eq} \simeq 1$ and a minimum electron Lorentz factor $\gamma_{\rm min} = 1$. The total synchrotron luminosity is most sensitive to these two parameters and our conservative values are chosen so as to ensure that $L^{\rm syn} \ll P_{\rm jet}$. The parameter $\gamma_{\rm max}$ determines the high-energy spectral cutoff. There are no observational constraints on this parameter so we simply set $\gamma_{\rm max} = 10^4$ in all cases. The jet length, $z_{\rm max}$, determines the synchrotron

Model	$M_{\rm bh}/M_\odot$	$L_{\rm Edd}$ $({\rm erg\,s^{-1}})$	$P_{\rm a}/L_{\rm Edd}$	$\dot{M}_{\rm a}$ $(M_\odot\,{\rm yr^{-1}})$	$\Gamma_{\rm j}$	$\theta_{\rm i}$ (deg)	δ	$L_{0.5-8\,{\rm keV}}$ $({\rm erg\,s^{-1}})$	$\nu L_\nu(5\,{\rm GHz})$ $({\rm erg\,s^{-1}})$
microblazar	5	6×10^{38}	1.0	1×10^{-7}	5	5	8.4	3×10^{39}	5×10^{31}
microquasar	20	3×10^{39}	1.0	5×10^{-7}	4	30	1.6	5×10^{39}	8×10^{31}

Table 1. Nominal model parameters resulting in apparent X-ray luminosities consistent with a ULX (see text for parameter definitions).

self-absorption turnover in the radio and X-ray bands. We keep this parameter at a fixed value of $10^9 r_{\rm g}$ so that it scales with $M_{\rm bh}$ and gives a radio self-absorption turnover at $\simeq 5\,{\rm GHz}$.

We differentiate between the microblazar and microquasar scenarios by using the spectral models defined in Sec. 2 with different values of the remaining free parameters: $M_{\rm bh}$, $\dot{M}_{\rm a}$ (parametrized by $P_{\rm a}/L_{\rm Edd}$), $\Gamma_{\rm j}$, and $\theta_{\rm i}$. Since a fraction $P_{\rm j}/P_{\rm a}$ of the total accretion power is channelled into a jet, values of $P_{\rm a}/L_{\rm Edd} > 1$ are allowed in the beaming models we consider. The value of $\Gamma_{\rm j}$ is somewhat constrained by the observation that persistent jets in Galactic XRBs appear to have $\Gamma_{\rm j} \lesssim 2$ (Fender 2005). On the other hand, if ULXs are at the extreme end of the XRB population, and if they are indeed small-scale versions of blazars and quasars, then we should not rule out the possibility that $\Gamma_{\rm j}$ could be higher. The most conservative parameter values that we find can give ULX luminosities are listed in Table 1. The corresponding predicted broadband spectra for the two models are shown in Figs. 2 and 3.

3.1 The microblazar model

For this model, we use $M_{\rm bh} = 5M_\odot$, $\Gamma_{\rm j} = 5$ and $\theta_{\rm i} = 5^\circ$, with the spectral model given by (13). This spectral model takes into account self-absorption of synchrotron radiation along the entire length of the jet. The resulting X-ray spectrum, Fig. 2, deviates significantly from a power-law as a result of relativistically beamed inverse Compton and (optically-thick) synchrotron emission. While this is somewhat difficult to reconcile with the generic featureless power-law fits to most ULX spectra, it is not at all clear whether spectra with $\lesssim 1000$ counts (e.g. in the *Chandra* sample, Swartz et al. 2004) have sufficient signal-to-noise to rule out Comptonization effects altogether (see Miller, Fabian & Miller 2006a). Indeed, new evidence has emerged from higher signal-to-noise *XMM-Newton* data for curvature in some ULX spectra above 2 keV ($\simeq 5\times10^{17}$)Hz (Stobbart et al. 2006). The spectral curvature has been interpreted in terms of thermal Comptonization from a warm, optically-thick corona (see e.g. Done & Kubota 2005; Goad et al. 2006), although this is difficult to reconcile with the lack of absorption features in the observed spectra to date.

The synchrotron optical depth is determined by the total jet length, $z_{\rm max}$. Here, $z_{\rm max} = 10^9 r_{\rm g}$ corresponds to $\sim 2\times10^{-4}\,{\rm pc}$. Increasing $z_{\rm max}$ shifts the X-ray self-absorption turnover in Fig. 2 from $\sim 10^{20}$ Hz to even higher frequencies; the highest energy synchrotron photons, produced near the jet base, have furthest to propagate to reach $z_{\rm max}$ and thus suffer the most self-absorption. At the same time, increasing $z_{\rm max}$ shifts the radio turnover to lower frequencies as more (optically-thin) radio-emitting jet plasma becomes available. The resulting radio spectrum is approximately flat near 10 GHz and steepens slightly towards the mm band. The opening diameter of the radio-emitting jet is $\sim 8\mu$ arcsec at $D \simeq 1\,{\rm Mpc}$, consistent with the appearance of a compact core. Despite the relativistic beaming effects, however, Fig. 2 shows that the radio spectral power falls short of the estimated $\sim 10^{24}{\rm erg\,s^{-1}\,Hz^{-1}}$ detectability threshold by two orders of magnitude. Whilst the radio emission can be increased by considering more extreme parameters (e.g. higher values of δ, $P_{\rm a}/L_{\rm Edd}$, or $f_{\rm eq}$), the resulting X-ray luminosities become implausibly high and the spectra become too hard.

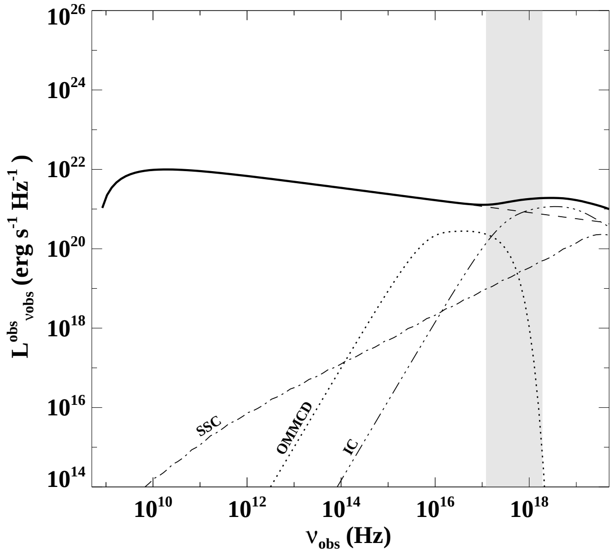

Figure 2. Apparent luminosity spectra predicted for the microblazar model ($M_{\rm bh} = 5M_\odot$, $\theta_{\rm i} < \phi_{\rm j}$). Linestyles are as follows: OMMCD spectrum (dotted), synchrotron (dashed), SSC (dot-dash), disk IC (dot-dot-dot-dash), and total disk plus jet spectrum (solid). The shaded region indicates the $0.5-8\,{\rm keV}$ X-ray band.

3.2 The microquasar model

One of the difficulties of the microblazar scenario is that it requires an implausibly large number of sources strongly beamed along different lines of sight for each source detected as a ULX (see e.g. the discussion in Sec. 6.2 of Davis & Mushotzky 2004). The microquasar scenario offers a more realistic prospect of addressing the observations and thus, it is of interest to determine how the emission properties of a jet change as the inclination angle increases. In particular, it is not immediately obvious whether a higher $M_{\rm bh}$ and $\dot{M}_{\rm a}$ can completely compensate for the decrease in Doppler boosting to give ULX X-ray luminosities.

We consider $\Gamma_{\rm j} = 4$ with $\theta_{\rm i} = 30°$, giving a jet Doppler factor $\delta = 1.6$. We also consider a higher mass, $M_{\rm bh} = 20 M_\odot$, which is a plausible upper limit for stellar-mass black holes formed from individual stars at solar metallicity (Fryer & Kalogera 2001). The spectral model we use for the microquasar case is given by (14) and the resulting spectrum is shown in Fig. 3. The most distinct difference between the microquasar and microblazar models is that the microquasar model predicts an optically-thin X-ray spectrum. Additionally, the X-ray spectrum is dominated by SSC emission, rather than IC emission and the spectrum is slightly flatter than the optically-thin synchrotron injection spectrum because the SSC photons in the $0.5 - 8\,$keV band result from seed photons in the optically-thin/thick turnover part of the synchrotron spectrum ($\sim 10^{15}\,$Hz in Fig. 3). As indicated in Table 1, the predicted X-ray luminosity for the microquasar model is comparable to that for the microblazar model for the parameters considered here.

The predicted radio spectral power is also approximately the same. The jet length, $z_{\rm max} = 10^9 r_{\rm g}$, corresponds to a physical size $\sim 10^{-3}\,$pc. For a source at $D \gtrsim 1\,$Mpc, the projected size of the radio-emitting jet is thus $\lesssim 0.2\,$mas. While this falls within reach of VLBI, the predicted radio emission of a microquasar ULX is simply too faint to expect a radio detection, let alone resolvable radio jet structure. The predicted specific luminosity at 1 GHz is $\sim 10^{22}\,{\rm erg\,s^{-1}\,Hz^{-1}}$ (comparable to that for the microblazar model), which corresponds to a flux density $\sim 10\mu$Jy at 1 Mpc. This is well below the detectability threshold and thus, the microquasar model is consistent with the majority of ULXs not being detected as radio sources. It also implies that the radio emission found associated with a few ULXs to date cannot be due to beamed synchrotron emission from a relativistic jet.

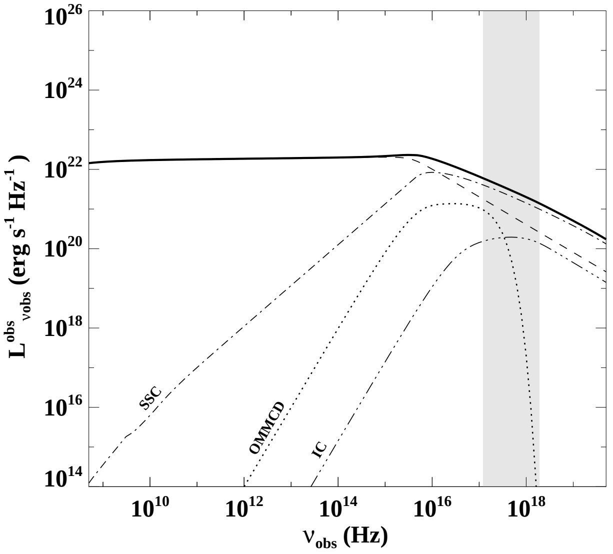

Figure 3. Apparent luminosity spectra predicted for the microquasar model ($M_{\rm bh} = 20 M_\odot$, $\theta_{\rm i} > \phi_{\rm j}$). Linestyles are the same as in Fig. 2 and the shaded region indicates the $0.5 - 8\,$keV X-ray band.

4 DISCUSSION

4.1 Disk properties

Our modified disk+jet model predicts *a priori* an anti-correlation between hard X-ray and soft X-ray spectral components. In our model, the hard (jet) component is beamed while the soft (disk) component is isotropic. Most ULXs appear to be dominated by a single power-law component in the X-ray band (Swartz et al. 2004). In many cases, the signal-to-noise ratio is not high enough for multi-component fitting, but even in sources with a high count rate, additional components (often attributed to thermal disk emission) contribute typically less than $10 - 20\,\%$ to the observed flux (Roberts & Colbert 2003; Miller et al. 2003, 2004; Krauss et al. 2005; Stobbart et al. 2006).

According to the currently prevailing interpretation of spectral states in Galactic XRBs (see McClintock & Remillard 2006, for a review), the low/hard state is accompanied by a steady jet and disk truncation at radii much larger than the innermost stable circular orbit (ISCO); this state occurs at low accretion rates ($\dot{M}_{\rm a} \lesssim 0.01 \dot{M}_{\rm Edd}$) and corresponding luminosities $\lesssim 0.01 L_{\rm Edd}$. It also implies a lower radiative efficiency in the inner region, often modelled as an advection-dominated flow. If ULXs are analogous to Galactic XRBs in their low/hard state (e.g. Winter et al. 2006), then extrapolation of their X-ray luminosities implies black hole masses $\gtrsim$ a few $\times 10^3 M_\odot$; it is still not known how such IMBHs can form and whether they are consistent with the observed ULX population.

We have instead suggested that ULXs behave more as if they are in a "high/hard" state, with $P_{\rm a} \sim L_{\rm Edd}$, even though $L_{\rm d} \ll P_{\rm a}$. In other words, with a high accretion rate and gravitational energy released all the way down to the ISCO, where it is mostly transferred to a steady jet or corona rather than being locally dissipated and radiated by the disk. This is different from the high/soft state, in which the jet appears to be suppressed. It also differs from the very high (or steep power-law) state that sometimes accompanies the transition in XRBs from the low/hard to high/soft state (Fender et al. 2004; McClintock & Remillard 2006); the very high state is characterized by sporadic radio ejections and an X-ray power-law spectrum steeper than those generally measured in bright ULXs. More generally, our OMMCD model offers a much needed alternative to the truncated disk model for an increasing number of sources characterized by a distinctive hard power-law component, together with evidence that the accretion flow extends all the way down to the ISCO (Ballantyne & Fabian 2005; Miller et al. 2006b).

We predict that, at the typical signal-to-noise level available for most X-ray spectra of ULXs (generally $\lesssim 1000$ counts even for the brightest sources), the modified disk spectral component may or may not be detectable depending on the relative importance of the jet (the parameter $P_{\rm j}/P_{\rm a}$ in our model) and that a low disk temperature may be the result of "jet cooling" rather than an implausibly high black hole mass. In the calculations presented here, we set $P_{\rm j}/P_{\rm a} = 0.9$ to produce a dominant nonthermal hard X-ray spectral component. To increase the relative contribution of the disk emission to $L_{\rm X}$, as appears to be required for some ULXs (e.g. Miller et al. 2003; Miller & Colbert 2004) we can decrease the ratio $P_{\rm j}/P_{\rm a}$ of accretion power being diverted into the jet. The observable disk quantity $T_{\rm in}$ (approximately corresponding to the annulus with the maximum flux contribution) also depends on the parameter q, which determines the radial profile of the magnetic torque responsible for jet formation, as defined in (4). We have set $q = 2.6$ in the calculations here. A steeper profile (e.g. $q \gtrsim 3$) removes more energy from small r and less energy from large r, thereby decreasing the X-ray brightness of the disk for a fixed $\dot{M}_{\rm a}$. Thus, to produce ULX spectra with a soft, thermal component in addition to the hard nonthermal component, as is sometimes observed, we can decrease $P_{\rm j}/P_{\rm a}$ in a suitable way to reproduce the observed fraction of radiative power emitted by the disk, and then vary q to increase or decrease $T_{\rm in}$. In general, the radial profile of the magnetic torque does not have to be a scale-free power-law; we intend to explore different profiles in future work. For practical purposes, the OMMCD spectrum can also be approximated by a standard disk with an empirical hardening factor $\xi < 1$ applied to the fitted colour temperature.

It is interesting to consider the implications of our model for the interpretation of spectral states in Galactic black hole XRBs. There is increasing evidence from detailed monitoring of individual sources (e.g. XTE J1550−564, Homan et al. 2001; Cyg X-1, Cadolle Bel et al. 2006; GX 339−4 Miller et al. 2006b) that changes in $\dot{M}_{\rm a}$ cannot solely be responsible for spectral state transitions and that an additional parameter is required to explain the full scope of observed spectral behaviour in XRBs. The additional parameter in our model is $P_{\rm j}/P_{\rm a}$, which measures the degree of magnetic coupling between disk and jet/corona. We expect that $P_{\rm j}/P_{\rm a}$ is approximately independent of $\dot{M}_{\rm a}$ for the following reason. From eqns. (3), (7) and (8), we have $P_{\rm j}/P_{\rm a} \propto r_{\rm i} B^{+}_{\phi}(r_{\rm i}) B^{+}_{z}(r_{\rm i})/(\dot{M}_{\rm a}\Omega(r_{\rm i})) \propto M^2 \dot{M}_{\rm a}^{-1} B^{+}_{\phi}(r_{\rm i}) B^{+}_{z}(r_{\rm i})$, since $r_{\rm i} \propto r_{\rm g}$. The magnetic field in the disk is amplified by the fluid shear and becomes dynamically important when $B^2 \sim \rho v^2$ (Kuncic & Bicknell 2004). Since $\rho \propto \dot{M}_{\rm a}$, we expect $P_{\rm j}/P_{\rm a} \propto M^p$, where $p = 2 - 3$, depending on the details of the accretion flow velocity and field amplification. Thus, to first-order, $P_{\rm j}/P_{\rm a}$ is independent of $\dot{M}_{\rm a}$ and is an increasing function of $M_{\rm bh}$. This implies that for a given $\dot{M}_{\rm a}$, more massive accretors can extract a larger fraction of total accretion power from the bulk fluid flow to produce more powerful jets.

Our model thus predicts that, contrary to the standard model for XRBs, steady jets need not necessarily be quenched in a high state and that sources such as ULXs which appear to be in a high *and* hard state are likely to have masses at the high-end of the XRB mass scale. This prediction is also supported by observations of AGN with $\dot{M}_{\rm a} \sim \dot{M}_{\rm Edd}$: radio-loud quasars tend to have black hole masses at the high end of the supermassive black hole mass scale (i.e. $M_{\rm bh} \sim 10^{8-9} M_\odot$) (e.g. Laor 2000; McLure & Jarvis 2004), while narrow-line Seyfert 1s (with $M_{\rm bh} \sim 10^{6-7} M_\odot$) are preferentially radio-quiet (see Greene, Ho & Ulvestad 2006; Komossa et al. 2006, and references therein).

Finally, it is worth reminding the reader here that we have worked in a Newtonian potential. Relativistic effects will change the radial disk flux profile at small r and may restrict the choice of q and $P_{\rm j}/P_{\rm a}$. This may provide further theoretical constraints on the ULX models considered here. A full relativistic derivation of the OMMCD model is beyond the scope of this paper, but will be presented elsewhere.

4.2 Jet properties

Our results show that beamed emission from a relativistic jet in a stellar-mass black hole binary system can produce an exceptionally bright X-ray source with a $0.5 - 8$ keV luminosity that is consistent with ULXs. The predicted X-ray spectra for the microblazar and microquasar scenarios have different distinguishing properties. In particular, the microblazar model (where the jet is viewed close to our line of sight) predicts a spectrum that becomes increasingly flatter towards hard X-ray energies in the $0.5 - 8$ keV bandpass, due to Comptonization effects (see Fig. 2). The observed spectrum of once-scattered disk photons rises to a peak just beyond the *Chandra*/*XMM-Newton* bandpass. The power-law component of this beamed inverse Compton emission falls in the gamma-ray band. It is difficult to rule out or confirm possible Comptonization effects from currently available ULX spectra (Miller et al. 2006a; see also the discussion in Gonçalves & Soria 2006). We do note, however, that some evidence for spectral curvature towards hard X-ray energies has recently emerged in *XMM-Newton* ULX spectra with high photon counts (Stobbart et al. 2006). The microquasar model, on the other hand, predicts a power-law X-ray spectrum due to beamed synchrotron self-Comptonization and thus offers a viable alternative to thermal Comptonization in a corona.

The predicted radio properties of the microblazar/quasar models are similar: the spectra are approximately flat near $5 - 10$ GHz and the specific radio luminosities are $\sim 10^{22}\,{\rm erg\,s^{-1}\,Hz^{-1}}$, corresponding to $\sim 10\mu$ Jy at $D \sim 1$ Mpc. How do these predicted radio properties compare to those observed? Very few radio counterparts of ULXs have been found so far, down to detection limits $\sim 10^{24}\,{\rm erg\,s^{-1}\,Hz^{-1}}$. The very low detection rates resulting from radio counterpart searches (e.g. Ghosh et al. 2005; Körding et al. 2005) strongly suggest that the vast majority of ULXs are intrinsically weak radio sources. Indeed, the ratio of radio-to-X-ray powers, $R_{\rm X} \equiv \nu L_\nu(5\,{\rm GHz})/L_{\rm X}$ (Terashima & Wilson 2003), predicted by our spectral modelling is $R_{\rm X} \simeq 10^{-8}$ for both the microblazar and microquasar cases (see Table 1). This is three orders of magnitude below the peak radio-to-X-ray power ratio observed in Galactic XRBs (Fender & Kuulkers 2001). Note, however, this also implies that a low measured value of $R_{\rm X}$ for ULXs with a radio counterpart cannot be used to rule out relativistic beaming (see e.g. Miller et al. 2004).

Our results imply that if the radio emission arises from synchrotron radiation in a relativistic jet, then ULXs should be too faint to be detected by current radio surveys. The few radio sources found associated with ULXs to date have specific radio powers $\sim 10^{25}\,{\rm erg\,s^{-1}\,Hz^{-1}}$ and steep radio spectra: $\alpha \sim -1$ for the ULX in NGC 5408 (Kaaret et al. 2003; Soria et al. 2006a), $\alpha \sim -(0.4 - 0.5)$ for the ULX in Ho II (Tongue & Westpfahl 1995; Miller et al. 2005) and $\alpha \sim -0.65$ for ULX 2 in NGC 7424 (Soria et al. 2006b). There is also evidence that the observed radio emission is marginally resolved (extended over $\sim 30 - 50\,\mathrm{pc}$) in two of those sources (NGC 5408 and Ho II) and for all the radio counterparts found so far, the ULX lies in an active star-forming region. The high flux, steep spectral index and possible spatial resolution suggest that those detected radio sources are not directly associated with a relativistic jet, but instead probably result from optically-thin emission from radio lobes or a radio SNR located near the ULX (Miller et al. 2005; Soria et al. 2006a,b) or even a combination of both (e.g. a scaled-up version of the Galactic source SS433; Fabrika 2004).

In the case of the radio lobe interpretation, the low detection rate can be attributed to the local ISM environment, which may be sufficiently less dense than the IGM that adiabatic losses are favoured over synchrotron losses in the jet lobes. This may explain the paucity of radio lobes in Galactic XRBs relative to those commonly seen in radio galaxies and quasars (Heinz 2002; Hardcastle 2005).

Finally, it is interesting to note that the theoretical radio and X-ray luminosities predicted by our relativistic beaming model for ULXs are remarkably consistent with the "fundamental plane" correlation between radio and X-ray emission and black hole mass (Gallo, Fender & Pooley 2003; Merloni, Heinz & di Matteo 2003; Falcke, Körding & Markoff 2004). This is surprising for two reasons. Firstly, the theoretical relation derived by Falcke et al. (2004) assumes optically-thin X-ray emission and neglects differences in radio and X-ray beaming (i.e. equivalent to our microquasar spectral model). It is not immediately obvious why the relation should hold if part of the X-ray emission is optically-thick, as is the case for our microblazar model. Secondly, the empirical relation found by Merloni et al. (2003), *viz.* $\log L_{\mathrm{R}} \simeq 0.60 \log L_{\mathrm{X}} + 0.78 \log M_{\mathrm{bh}} + 7.33$ (where L_{R} denotes radio power at the observing frequency, νL_ν), strictly only holds for sources in a low state; it is still unclear to what extent it holds or breaks down for sources which are in a high state (see Körding, Falcke & Corbel 2006).

5 CONCLUSIONS

Current observational evidence suggests that most of the X-ray emission from ULXs does not come directly from the accretion disk, which is either not directly visible, or colder than in bright stellar-mass XRBs. We have used a coupled disk+jet theoretical framework to explain why most of the energy is not directly radiated from the disk, and to test whether a relativistic beaming scenario (microblazar or microquasar) is consistent with the observed X-ray and radio spectra. Our main conclusions can be summarized as follows:

1. The accretion disk can be substantially modified by the presence of a magnetized jet; this gives rise not only to a modified disk spectrum, but also to a decrease in the peak colour temperature (T_{in}) of the inner disk for a fixed mass accretion rate. The modified disk+jet model thus predicts an anticorrelation between the relative importance of hard (jet) and soft (disk) X-ray spectral components.
2. We confirm that both the stellar-mass microblazar and microquasar scenarios can produce apparent X-ray luminosities in the ULX regime ($L_{0.5-8\,\mathrm{keV}} \gtrsim 2 \times 10^{39}\,\mathrm{erg\,s^{-1}}$). A general feature of our disk+jet model is that it can produce hard, nonthermal X-ray spectra that are analogous to the classic low/hard spectral state in XRBs, but applicable to high mass accretion rates ($\dot{M}_{\mathrm{a}} \sim \dot{M}_{\mathrm{Edd}}$) and, therefore, high luminosity sources. In our model, a magnetic torque provides the mechanism for transferring a substantial fraction of the total accretion power $P_{\mathrm{a}} \sim L_{\mathrm{Edd}}$ from the disk to the jet (i.e. $P_{\mathrm{j}} \sim L_{\mathrm{Edd}}$). Our spectral model for the microblazar predicts a substantially hardened X-ray spectrum due to strong beaming and Comptonization effects. The microquasar model, on the other hand, produces a featureless power-law spectrum.
3. Both the microblazar and microquasar models predict that, despite the beaming effects, ULXs are intrinsically weak radio emitters. This result is compatible with the overwhelming excess of non-detections over detections in ULX radio observations to date. Neither of the beaming models are consistent with the few ULX radio counterpart detections reported to date. We therefore conclude that the observed radio emission cannot be attributed to beamed synchrotron emission in a relativistic jet. We suggest it is likely due to radio lobes or a radio SNR. We predict that deeper observations around 20 GHz should in principle detect a change in radio spectral index, thus resolving the direct jet contribution from the lobe emission.

In this paper, we have restricted ourselves to modelling beamed emission from accreting black holes with masses in the known stellar-mass range ($5 - 20\,M_\odot$). If IMBHs exist, it is legitimate to assume (based on the stellar-mass and supermassive black hole analogies) that some IMBHs can also possess relativistic jets. If some IMBHs have beamed emission, then we would expect to find at least a few milliblazars and milliquasars with apparent X-ray luminosities in excess of $10^{41}\,\mathrm{erg\,s^{-1}}$. Such sources have not yet been seen.

The disk+jet model we have proposed here requires that more gravitational energy is channelled into a jet than is radiated by a disk, at least during some phases of accretion. At low or moderate accretion rates, new evidence of significant feedback onto the ISM surrounding accreting black holes indicates that jets can indeed carry away much more energy than is radiated by the disk (e.g. Owen et al. 2000; Churazov et al. 2002). At accretion rates approaching the Eddington rate, however, observations suggest that jets are quenched in Galactic XRBs (e.g. Fender et al. 2004) and in low-mass AGN (e.g. Greene et al. 2006), but can persist in AGN with high black hole masses (e.g. Laor 2000; McLure & Jarvis 2004). Our model predicts that the fractional accretion power chanelled into jets scales with black hole mass and is independent of the mass accretion rate. It therefore predicts that jets can be the dominant energy carrier, even at high ($\sim$ Eddington) accretion rates. If this is correct, it should be possible to find evidence of relativistic jet emission also in some other accreting black hole sources in which the hard X-ray component has perhaps been misinterpreted as, for example, thermal Comptonization in a corona.

ACKNOWLEDGMENTS

ZK thanks K. Wu, R. Hunstead and E. Sadler for useful discussions and acknowledges support from a University of Sydney Research and Development Grant. RS acknowledges support from a University of Sydney Denison Grant and an OIF Marie Curie Fellowship. GVB acknowledges support for this research from Australian Research Council Discovery Project 0345983.

REFERENCES

Ballantyne, D. R., Fabian, A. C. 2005, ApJ, 622, L97

Begelman, M. C., Blandford, R. D., Rees, M. J. 1984, Rev. Mod. Phys., 56, 255

Blair, W. P., Fesen, R. A., Schlegel, E. M. 2001, AJ, 121, 1497

Blandford, R. D., Königl, A. 1979, ApJ, 232, 34

Blandford, R. D., Payne, D. G. 1982, MNRAS, 199, 883

Blumenthal, G. R., Gould, R. J., 1970, Rev. Mod. Phys., 42, 237

Cadolle Bell, M., et al. 2006, A&A, 446, 591

Celotti, A., Fabian, A. C. 1993, MNRAS, 264, 228

Celotti, A., Kuncic, Z., Rees, M. J., Wardle, J. F. C. 1998, MNRAS, 293, 288

Charles, P. 1998, in Theory of Black Hole Accretion Disks, eds. M. A. Abramowicz, G. Bjornsson & J. E. Pringle, Cambridge Univ. Press, 1

Churazov, E., Sunyaev, R., Forman, W., Böhringer, H. 2002, MNRAS, 332, 729

Colbert, E. J. M., Mushotzky, R. F. 1999, ApJ, 519, 89

Crummy, J., Fabian, A. C., Gallo, L., Ross, R. R. 2005, MNRAS, in press

Davis, D. S., Mushotzky, R. F. 2004, ApJ, 604, 653

Done, C., Kubota, A. 2005, MNRAS, submitted (astro-ph/0511030)

Esin, A. A., McClintock, J. E., Narayan, R. 1997, ApJ, 489, 865

Fabian, A. C., Ross, R. R., Miller, J. M. 2004, MNRAS, 355, 359

Fabrika, S. 2004, Astrophys. Sp. Phys. Rev., 12, 1

Fabrika, S., Mescheryakov, A. 2001, in Galaxies and their Constituents at the Highest Angular Resolution, Proc. IAU Symp. 205, ed. R. T. Schilizzi, 268

Falcke, H., Körding, E., Markoff, S. 2004, A&A, 414, 895

Fender, R. P. 2005, in Compact Stellar X-ray Sources, eds. W. H. G. Lewin and M. van Der Klis, astro-ph/0303339.

Fender, R., Belloni, T. 2004, ARAA, 24, 317

Fender, R., Kuulkers, E. 2001, MNRAS, 324, 923

Fender, R. P., Belloni, T. M., Gallo, E. 2004, MNRAS, 355, 1105

Gallo, E., Fender, R. P., Pooley, G. G. 2003, MNRAS, 344, 60

Fryer, C. L., Kalogera, V. 2001, ApJ, 554, 548

Georganopoulos, M., Aharonian, F. A., Kirk, J. G. 2002, A&A, 388, L25

Ghisellini, G., Celotti, A. 2001, MNRAS, 327, 739

Ghisellini, G., Maraschi, L., Treves, A., 1985, A&A, 146, 204

Ghisellini, G., Padovani, P., Celotti, A., Maraschi, L., 1993, ApJ, 407, 65

Ghosh, K. K., Swartz, D. A., Tennant, A. F., Wu, K., Saripalli, L. 2005, ApJ, 623, 815

Goad, M. R., Roberts, T. P., Reeves, J. N., Uttley, P. 2006, MNRAS, 365, 191

Gonçalves, A. C., Soria, R. 2006, MNRAS, in press.

Greene, J. E., Ho, L. C., Ulvestad, J. S. 2006, ApJ, 636, 56.

Gutiérrez, C. M., López-Corredoira, M. 2005, ApJ, 622, L89

Hardcastle, M. J. 2005, A&A, 434, 35

Heinz, S. 2002, A&A, 388, L40

Homan, J., et al. 2001, ApJS, 132, 377

Irwin, J. A., Bregman, J. N., Athey, A. E. 2004, ApJ, 601, L143

Kaaret, P., Corbel, S., Prestwich., A. H., Zezas, A. 2003, Science, 299, 365

Kaaret, P., Ward, M. J., Zezas, A. 2004, MNRAS, 351, L83

King, A. R. 2004, MNRAS, 347, L18

King, A. R., Davies, M. B., Ward, M. J., Fabbiano, G., Elvis, M. 2001, ApJ, 552, L109

King, A. R., Dehnen, W. 2005, MNRAS, 357, 275

King, A. R., Pounds, K. A. 2003, MNRAS, 345, 657

Komossa, S., et al. 2006, ApJ, submitted (astro-ph/0603680)

Königl, A., 1981, ApJ, 243, 700

Körding, E., Colbert, E., Falcke, H. 2005, A&A, 436, 427

Körding, E., Falcke, H., Corbel, S. 2006, A&A, in press (astro-ph/0603117)

Körding, E., Falcke, H., Markoff, S. 2002, A&A, 382, L13

Krauss, M. I., Kilgard, R. E., Garcia, M. R., Roberts, T. P., Prestwich, A. H. 2005, ApJ, 630, 228

Kronberg, P. P., Sramek, R. A. 1985, Science, 227, 28

Kubota, A., et al. 2001, ApJ, 547, L119

Kubota, A., Done, C., Makishima, K., 2002, MNRAS, 337, L11

Kuncic, Z., Bicknell, G. V. 2004, ApJ, 616, 669

Laor, A. 2000, ApJ, 543, L111

La Parola, V., Peres, G., Fabbiano, G., Kim, D. W., Bocchino, F. 2001, ApJ, 556, 47

Lind, K. R., Blandford, R. D., 1985, ApJ, 295, 358

Liu, J.-F., Bregman, J. N., Seitzer, P. 2002, ApJ, 580, L31

Liu, J.-F., Bregman, J. N., Seitzer, P. 2004, ApJ, 602, 249

Makishima, K., et al. 2000, ApJ, 535, 632

Markoff, S., Nowak, M. A. 2004, ApJ, 609, 972

Markoff, S., Falcke, H., Fender, R. 2001, A&A, 372, L25

Markoff, S., Nowak, M., Corbel, S., Fender, R., Falcke, H. 2003, A&A, 397, 645

McClintock, J. E., Remillard, R. A. 2006, in Compact Stellar X-ray Sources, eds. W. H. G. Lewin, M. van der Klis, Cambridge Univ. Press (astro-ph/0306213)

McClure, R. J., Jarvis, M. J. 2004, MNRAS, 353, L45

Merloni, A., Fabian, A. C., Ross, R. R. 2000, MNRAS, 313, 193

Merloni, A., Heinz, S., di Matteo, T. 2003, MNRAS, 345, 1057

Miller, M. C., Colbert, E. J. M., 2004, International Journal of Modern Physics D, 13, 1-64

Miller J. M., Fabbiano, G., Miller M.C., Fabian A. C. 2003, ApJ, 585, L37

Miller J. M., Fabian A. C., Miller M. C. 2004, ApJ, 607, 931

Miller J. M., Fabian A. C., Miller M. C. 2006a, MNRAS, submitted (astro-ph/0512552)
Miller J. M., et al. 2006b, ApJ, submitted (astro-ph/0602633)
Miller N. A., Mushotzky R. F., Neff S. G., 2005, ApJ, 623, L109
Mizuno, T., Kubota, A., Makishima, K. 2001, ApJ, 554, 1282.
Owen, F. N., Eilek, J. A., Kassim, N. E. 2000, ApJ, 543, 611.
Punsly, B., Tingay, S. J. 2005, ApJ, 633, L89
Roberts, T. P., Colbert, E. J. M. 2003, MNRAS, 341, L49
Schwartz. D. A. et al. 2006, ApJ, in press (astro-ph/0601632)
Shakura, N. I., Sunyaev, R. A. 1973, A&A, 24, 337
Shrader, C. R., Titarchuk, L. 2003, ApJ, 598, 168
Soria, R., Motch, C., 2004, A&A, 422, 915
Soria, R., Fender, R. P., Hannikainen, A. M., Read, A. M., Stevens, I. R. 2006, MNRAS, submitted
Soria, R., Kuncic, Z., Broderick, J., Ryder, S. D. 2006, MNRAS, submitted
Stobbart, A.-M., Roberts, T. P., Wilms, J. 2006, MNRAS, in press
Strickland, D. K. et al., 2001, ApJ, 560, 707
Strohmayer, T. E., Mushotzky, R. F. 2004, ApJ, 586, L61
Swartz, D. A., Ghosh, K. K., Tennant, A. F., Wu, K. 2004, ApJS, 154, 519
Terashim, Y., Wilson, A. S. 2003, ApJ, 583, 145 Tongue, T. D., Westpfahl, D. J. 1995, AJ, 109, 2462
Tongue, T. D., Westpfahl, D. J. 1995, AJ, 109, 2462
van Dyk, S. D., Sramek, R. A., Weiler, K. W., Hyman, S. D., Virden, R. E. 1994, ApJ, 425, L77
Winter, L. M., Mushotzky, R. F., Reynolds, C. S. 2006, ApJ, submitted (astro-ph/0512480)
Zampieri et al. 2004, ApJ, 603, 523

This paper has been typeset from a TEX/ LATEX file prepared by the author.